THE JOURNAL OF BIOLOGICAL CHEMISTRY
Vol. 273, No. 29, Issue of July 17, pp. 18122–18129, 1998

*Printed in U.S.A.*

# Aerolysin Induces G-protein Activation and $Ca^{2+}$ Release from Intracellular Stores in Human Granulocytes*

(Received for publication, December 22, 1997, and in revised form, April 6, 1998)

**Karl-Heinz Krause‡, Marc Fivaz§, Antoinette Monod‡, and F. Gisou van der Goot§¶**

*From the ‡Infectious Diseases Division, University Hospital, 1211 Geneva 14, Switzerland and the §Department of Biochemistry, University of Geneva, 30 quai E. Ansermet, 1211 Geneva 4, Switzerland*

**Aerolysin is a pore-forming toxin that plays a key role in the pathogenesis of *Aeromonas hydrophila* infections. In this study, we have analyzed the effect of aerolysin on human granulocytes (HL-60 cells). Proaerolysin could bind to these cells, was processed into active aerolysin, and led to membrane depolarization, indicating that granulocytes are potential targets for this toxin. Fura-2 measurements were used to analyze the effect of aerolysin on cytosolic [$Ca^{2+}$] homeostasis. As expected for a pore-forming toxin, aerolysin addition led to $Ca^{2+}$ influx across the plasma membrane. In addition, the toxin triggered $Ca^{2+}$ release from agonist and thapsigargin-sensitive intracellular $Ca^{2+}$ stores. This $Ca^{2+}$ release was independent of the aerolysin-induced $Ca^{2+}$ influx and occurred in two kinetically distinct phases: an initial rapid and transient phase and a second, more sustained, phase. The first, but not the second phase was sensitive to pertussis toxin. Activation of pertussis toxin-sensitive G-proteins appeared to be a consequence of pore formation, rather than receptor activation through aerolysin-binding, as it: (i) was not observed with a binding competent, insertion-incompetent aerolysin mutant, (ii) had a marked lag time, and (iii) was also observed in response to other bacterial pore-forming toxins (staphylococcal α-toxin, streptolysin O) which are thought to bind to different receptors. G-protein activation through pore-forming toxins stimulated cellular functions, as evidenced by pertussis toxin-sensitive chemotaxis. Our results demonstrate that granulocytes are potential target cells for aerolysin and that in these cells, $Ca^{2+}$ signaling in response to a pore-forming toxin involves G-protein-dependent cell activation and $Ca^{2+}$ release from intracellular stores.**

Aerolysin is a pore-forming toxin secreted by the human pathogen *Aeromonas hydrophila* and has been shown to be an important virulence factor produced by this bacterium (1–5). *A. hydrophila* has been implicated in a variety of diseases ranging from gastroenteritis to deep wound infection and septicemia. The importance of aerolysin in the pathogenicity of the bacterium is best illustrated by the fact that immunization against the toxin leads to protection toward the bacterium.

The toxin is secreted by *A. hydrophila* as a dimeric inactive precursor (6, 7) which can be activated by proteolytic cleavage of a C-terminal peptide (8, 9). The toxin as well as the protoxin interact with the target cell by binding to specific receptors (10–14). At present all identified receptors were found to be GPI[1] anchored. However, different receptors were found on different cells types and a given cell type was found to have more then one receptor. For example, aerolysin was shown to bind to Thy-1 as well as other GPI-anchored proteins on T-lymphocytes, to Thy-1 and contactin in mouse brain (11, 13), to VSG from Trypanosomes (13), to an 47-kDa receptor on rat erythrocytes (12) and to mainly an 80-kDa receptor on baby hamster kidney cells (14). Binding was shown to be determined both by the protein moiety and the olisaccharides of the anchor (13). Binding to the cell surface presumably leads to a local increase in toxin concentration thereby enabling aerolysin to polymerize into a heptameric complex that inserts into the membrane and forms a water-filled channel (6, 15–18). Cells such as erythrocytes, that are unable to cope with such membrane damage, undergo osmotic lysis. In nucleated mammalian cells, the mechanisms leading to cell death appear to be more complex. We have indeed recently found that subnanomolar doses of aerolysin do not induce lysis of baby hamster kidney cells (14). Permeabilization but not disruption of the plasma membrane was observed followed by selective vacuolation of the endoplasmic reticulum (14). Only several hours later could a loss of plasma membrane integrity be observed. It is at present not clear whether the pores formed by the toxin at the plasma membrane are the sole cause of the observed effects. These findings, however, do suggest that aerolysin may trigger a cascade of events from the plasma membrane.

In this study, we have analyzed the effects of aerolysin on human granulocytes. We show that, in addition to formation of pores in the plasma membrane, aerolysin triggered, through activation of a pertussis toxin-sensitive G-protein, chemotaxis, and release of $Ca^{2+}$ from intracellular stores.

## EXPERIMENTAL PROCEDURES

*Materials*—Cell culture media were obtained from Life Technologies, Inc. (Paisley, Scotland), U73122 from Calbiochem (La Jolla, CA), and $DiSC_3(5)$, PBFI, and fura-2/AM from Molecular Probes (Eugene, OR). All other chemicals were purchased from Sigma or Fluka. The "$Ca^{2+}$-free medium" contained: 143 mM NaCl, 6 mM KCl, 1 mM $MgSO_4$, 5.6 mM glucose (0.1%), 20 mM HEPES pH 7.4, and 0.1 mM EGTA. The "$Ca^{2+}$ medium" consisted of $Ca^{2+}$-free medium supplemented with 1 mM $CaCl_2$.

*Culture of HL-60 Cells*—HL-60 cells were cultured in RPMI 1640 medium supplemented with 10% heat-inactivated fetal calf serum, penicillin (50 units/ml), streptomycin (50 μg/ml), and L-glutamine (2 mM) at 37 °C in a humidified atmosphere of 5% $CO_2$, 95% air. Granulocytic differentiation was initiated by addition of dimethyl sulfoxide ($Me_2SO$) (final concentration 1.3% for 3 days, then 0.65% for 1 or 2 days).

* This work was supported by Swiss National Science Foundation Grants 3100-04 5891.95/1 (to K-H. K.) and 3100-049195.96/1 (to G. v. d. G). The costs of publication of this article were defrayed in part by the payment of page charges. This article must therefore be hereby marked "*advertisement*" in accordance with 18 U.S.C. Section 1734 solely to indicate this fact.

¶ To whom correspondence should be addressed. Tel./Fax: 41-022-702-6414; E-mail: Gisou.vandergoot@biochem.unige.ch.

[1] The abbreviations used are: GPI, glycosylphosphatidylinositol; PAGE, polyacrylamide gel electrophoresis; PLC, phospholipase C; $Ins(1,4,5)P_3$, inositol 1,4,5-trisphosphate; $Me_2SO$, dimethyl sulfoxide; ER, endoplasmic reticulum; fMLP, fMet-Leu-Phe; PBFI, $K^+$-binding benzofuran isophthalate.

*Proaerolysin Purification*—Wild type and variant proaerolysins were purified as described previously (19). Concentrations were determined by measuring the optical density (O.D.) at 280 nm, considering that a 1 mg/ml sample has an O.D. of 2.5 (20). Proaerolysin was labeled with $^{125}I$ using IODO-GEN reagent (Pierce) according to the manufacturers recommendations. $^{125}I$-Proaerolysin was separated from the free iodine by gel filtration on a PD10-G25 column (Pharmacia, Sweden) equilibrated with phosphate-buffered saline. We consistently obtained a specific activity of about $2 \times 10^6$ cpm/$\mu$g of proaerolysin. $^{125}I$-Proaerolysin ran as a single band on an SDS gel. Aerolysin was obtained by treating proaerolysin with trypsin at a protein to enzyme ratio of 1/20 (mol:mol) for 10 min at room temperature. After which a 10-fold excess of trypsin inhibitor was added.

*Proaerolysin Binding Experiments*—HL-60 granulocytes at a concentration of $2 \times 10^6$ cells/ml in $Ca^{2+}$ medium were incubated with $^{125}I$-proaerolysin for 25 min at 4 °C, spun down in a table top cell centrifuge for 8 min at 1600 rpm, resuspended in the same volume of buffer. The last washing step was performed twice. In competition experiments, $^{125}I$-proaerolysin and the unlabeled wild type or mutant toxin were added to the cells simultaneously. For SDS-PAGE analysis, cells were briefly sonicated with a tip sonicator in sample buffer. SDS-PAGE was performed as described by Laemmli (21).

*Membrane Potential Measurements*—HL-60 granulocytes were washed once and resuspended in buffer containing 20 mM HEPES pH 7.4, 143 mM NaCl, 5 mM KCl, 1 mM $MgSO_4$, 1 mM $CaCl_2$, 5.6 mM glucose, to a final density of $3 \times 10^6$ cells/ml. DiS-$C_3$(5) (100 $\mu$M in $Me_2SO$) was added to a final concentration of 200 nM. Membrane incorporation of the dye was monitored spectrofluorimetrically using a Photon Technology International fluorometer equipped with a thermostated cuvette holder (excitation 625 nm; emission 670 nm; 10 nm slits). After reaching a steady state fluorescence, the toxin was added. Maximal depolarization was obtained at the end of each experiment by adding pre-mixed valinomycin and nigericin to final concentrations of 2 and 5 $\mu$M, respectively (22). Single fluorescent traces were expressed as the ratio $I(t)/I_{max}$, *i.e.* fluorescence intensity at a given time over maximal fluorescence intensity.

*Measurements of Intracellular $K^+$ Concentration*—HL-60 granulocytes were washed once and resuspended in loading medium, containing 20 mM HEPES pH 7.4, 5.6 mM glucose, 143 mM NaCl, 6 mM KCl, 1 mM $MgSO_4$, 1 mM $CaCl_2$, 0.5% bovine serum albumin, and 0.25 mM sulfinpyrazone, to a final density of $20 \times 10^6$ cells/ml (22). Cells were incubated with the cell-permeant form of the $K^+$-binding benzofuran isophtalate dye PBFI-AM (stock solution in $Me_2SO$ in presence of pluronic acid F-127, final concentrations of 5 $\mu$M PBFI and 0.02% F-127) for 30 min at 37 °C, followed by 30 min at room temperature, washed once and resuspended in the same buffer, in the absence of bovine serum albumin, to a final density of $2 \times 10^6$ cells/ml. Fluorescence measurements were performed using a Photon Technology International fluorometer. The excitation and emission wavelengths were 343 and 460 nm, respectively (37 °C). Variations of intracellular $K^+$ contents were expressed as a fraction of PBFI maximal intensity.

*Measurements of Ethidium Homodimer-1 and Ethidium Bromide Cell Entry*—HL-60 granulocytes were washed once and resuspended in 20 mM HEPES pH 7.4, 5.6 mM glucose, 143 mM NaCl, 6 mM KCl, 1 mM $MgSO_4$, 1 mM $CaCl_2$, to a final density of $20 \times 10^6$ cells/ml. Ethidium homodimer-1 (stock solution 2 mM in $Me_2SO$/water, 1:4) or ethidium bromide (stock solution 10 mg/ml in water) were added to a final concentration of 6 nM and 100 $\mu$M, respectively. Aerolysin-induced ethidium homodimer-1 or ethidium bromide entry was monitored by measuring the increase of fluorescence intensity at 600 nm, upon excitation at 500 or 340 nm, respectively. Single fluorescent traces were normalized to maximal fluorescence obtained by the addition of 1% Triton X-100.

*Measurement of Cytosolic Free $Ca^{2+}$ Concentrations*—$[Ca^{2+}]_c$ was measured with the fluorescent $Ca^{2+}$ indicator fura-2. Cells ($2 \times 10^7$/ml) suspended in $Ca^{2+}$ medium containing 0.1% bovine serum albumin were loaded for 45 min at 37 °C with 2 $\mu$M fura-2/AM, then diluted to $10^7$/ml and kept on ice. Just before use, a sample of loaded cells ($2 \times 10^6$/ml) was centrifuged and resuspended in the desired medium. Fluorescence measurements were performed on a Perkin-Elmer fluorometer (LS3, Perkin-Elmer), thermostated at 37 °C. Excitation and emission wavelengths were 340 and 505 nm, respectively. Calibration was performed for each cuvette by sequential addition of 2 mM $Ca^{2+}$ (for $Ca^{2+}$-free medium), 1 $\mu$M ionomycin to measure $Ca^{2+}$ saturated fura-2 ($F_{max}$), followed by 24 mM EGTA, 75 mM Tris, pH 9.3, and 0.1% Triton X-100 to measure $Ca^{2+}$ free fura-2 ($F_{min}$). A relatively small leakage of fura-2 occurred in cells exposed to aerolysin (see "Results"). Results are shown as relative fura-2 fluorescence, normalized with respect to the maximal fluorescence (=100%) and minimal fluorescence (=0%) values obtained through the calibration procedure.

*Measurement of $Mn^{2+}$ and $Ni^{2+}$ Entry*—At an excitation wavelength of 360 nm, fura-2 fluorescence is $Ca^{2+}$ independent, the fluorescence of the probe is, however, quenched by several divalent cations. In this study, we used this feature of the probe to study entry of $Mn^{2+}$ and $Ni^{2+}$ in response to aerolysin independently from changes in $[Ca^{2+}]_c$. Cell-associated fluorescence before addition of the respective divalent cation was defined as 100% fluorescence. For the quantitation of the $Mn^{2+}$ influx at different times after aerolysin addition, we proceeded as described previously (23). Briefly, the percentage of fluorescence quenching that occurred within 1 min after $Mn^{2+}$ addition was determined. The relatively small fraction of the fluorescence quenching that was due to the presence of extracellular fura (see below) was subtracted. The emission wavelength was 505 nm.

*Determination of Extracellular Fura-2*—To determine the amount of extracellular fura-2, we exposed fura-2-loaded cells for various times to aerolysin, followed by the addition of 25 $\mu$M $Mn^{2+}$ and, 1 min later, 100 $\mu$M of the heavy metal chelator diethylenetriaminepentaacetic acid. Under these conditions, the fraction of the $Mn^{2+}$-induced fluorescence quenching that is immediately reversible after addition diethylenetriaminepentaacetic acid is a direct measure of extracellular fura-2 (23).

*Chemotaxis Assay*—For the chemotaxis assay, a Transwell® chemotaxis chamber (6.5 mm diameter, 3 $\mu$m pore size, Corning Costar Corp., Cambridge, MA) was used. In this system, the cell reservoir (=upper chamber) is separated from the target chamber (=lower chamber) by a microporous membrane. The cell reservoir contained $10^6$ cells in 100 $\mu$l of $Ca^{2+}$ buffer with 0.1% bovine serum albumin. The target chamber contained the indicated concentration of chemoattractant or the appropriate solvent control in 500 $\mu$l of $Ca^{2+}$ buffer with 0.1% bovine serum albumin. Chemotaxis was allowed to occur over a period of 90 min in an $CO_2$ (5%) and temperature (37 °C)-controlled incubator. Cells in the target chamber were counted. Results are expressed as cells recovered in the target chamber (% of cells that were initially added in the cell reservoir).

## RESULTS

*Binding to HL-60 Cells*—As a first step in the characterization of the interaction of proaerolysin with myeloid cells, we have investigated whether proaerolysin was able to bind to HL-60 promyelocytes and HL-60 granulocytes. Cells were incubated with 1 nM proaerolysin at 4 °C for 10 min, washed, sedimented, and analyzed by SDS-PAGE followed by Western blot analysis for the presence of the toxin. Both wild type proaerolysin as well as a double cysteine mutant, G202C/I445C (see below), were able to bind to both types of HL-60 cells (not shown).

To investigate whether binding of proaerolysin was specific, we have analyzed whether radiolabeled and unlabeled proaerolysin could compete for binding to HL-60 cells. Binding of radiolabeled proaerolysin (4 nM) to both promyelocytic and granulocytic HL-60 could be inhibited by more than 80% by the presence of a 100-fold excess of unlabeled toxin (0.4 $\mu$M), indicating the presence of a limited number of binding sites. Binding of radiolabeled wild type toxin could also be inhibited, to the same extend, by unlabeled G202C/I445C mutant toxin, indicating that both forms of the toxin bind to the same sites.

These observations suggest that aerolysin binds to a limited number of sites on HL-60 cells. Using a previously described proaerolysin overlay assay (14), we could identify 4 proaerolysin-binding proteins (not shown). Binding to these proteins could be inhibited by 70% by treating the cells with the phosphatidylinositol-specific phospholipase C indicating that these putative receptors were GPI anchored (not shown). These four proteins remain to be identified. We could, however, exclude that binding occurred via Thy-1, which was shown to be a receptor for aerolysin on T-lymphocytes (11), since HL-60 do not express this protein to any significant extent (24). The presence of multiple receptors on HL-60 granulocytes is reminiscent of what was observed in rat brain, were at least two receptors were found, Thy-1 and contactin (13), and on baby hamster kidney cells were three putative GPI-anchored recep-

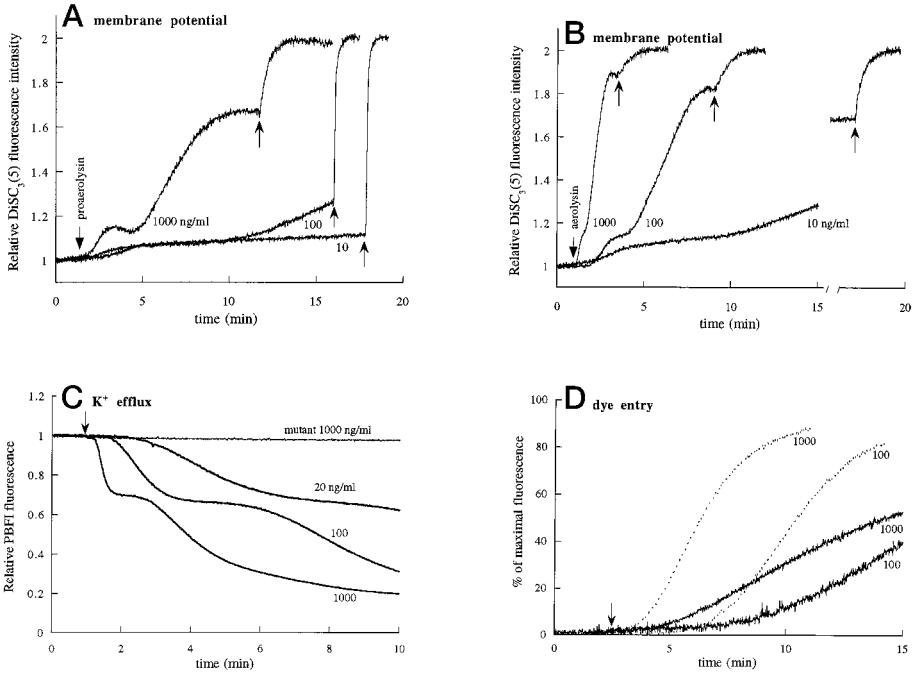


FIG. 1. **Aerolysin selectively permeabilizes the plasma membrane of HL-60 granulocytes.** *A* and *B*, changes induced by proaerolysin (*A*) and trypsin-activated aerolysin (*B*) of the fluorescence of the membrane potential sensitive probe $DiSC_3(5)$ after uptake by HL-60 granulocytes. *C*, the aerolysin induced change in intracellular $K^+$ was followed by monitoring the changes of PBFI fluorescence after loading the cells with this dye as described under "Experimental Procedures." Trypsin-activated aerolysin was added at the time indicated by an *arrow*. *D*, aerolysin induced influx in ethidium bromide (*dashed line*) and ethidium homodimer-1 (*full line*). Trypsin-activated aerolysin was added at the time indicated by an *arrow*.

tors were seen of, respectively, 140, 80, and 30 kDa, the 80-kDa protein being the major proaerolysin-binding protein (14).

*Aerolysin Induces Plasma Membrane Depolarization in HL-60 Granulocytes*—To investigate whether HL-60 granulocytes are sensitive to aerolysin, we have analyzed the effect of the toxin on membrane potential using the fluorescent probe $DiSC_3(5)$ which has been widely used for this purpose (25). As shown in Fig. 1*A*, proaerolysin led to depolarization of the granulocytes with kinetics that were dose-dependent. As suspected, a marked increase in the rate of depolarization was observed when activating the protoxin prior to the addition to the cells (Fig. 1*B*). As shown in Fig. 1*C*, depolarization was in part due to the efflux of $K^+$. As a control, we tested the hemolytically inactive mutant of aerolysin, G202C/I445C. This mutant contains two engineered cystein residues that form a disulfide bridge between the propeptide and the mature toxin (20). Even after trypsin activation, this mutant is unable to lyse erythrocytes presumably because it cannot oligomerize. Also G202C/I445C did not induce $K^+$ efflux from HL-60 granulocytes. Surprisingly, depolarization of HL-60 granulocytes as well as $K^+$ efflux followed two-step kinetics for reasons that remain to be established. In contrast, kinetics of membrane depolarization induced by the thiol-activated toxin streptolysin O were monophasic (not shown).

The observed $K^+$ efflux and membrane depolarization were not due to lysis of the cells as illustrated by the fact that most cells still exclude ethidium homodimer-1 after 10 min (Fig. 1*D*). Faster kinetics of entry were observed with the smaller dye ethidium bromide indicating that a sieving mechanism was taking place. This observation suggests that the dye enters the cells through the aerolysin pore and not through a breach in the plasma membrane since in the latter case no discrimination in size would be expected. We can therefore conclude that aerolysin led to selective permeabilization of the plasma membrane and not to cell lysis within the time frame of the present experiments. Aerolysin was also able to induce membrane depolarization and $K^+$ efflux in HL-60 promyelocytes, although the kinetics were dramatically slower then those observed for granulocytes (not shown).

Since membrane depolarization could be observed not only when treating the cells with aerolysin but also with proaerolysin, albeit at far slower rate, we investigated whether HL-60 granulocytes expressed proteases able to process the protoxin. As shown in Fig. 2, although the protoxin added to the cells showed no sign of contamination by aerolysin (*lane a*), a lower molecular weight form corresponding to aerolysin could be observed upon interaction with the granulocytes. A higher molecular weight band could also be observed upon incubation at 37 °C corresponding to the aerolysin heptamer (Fig. 2). These results agree well with our previous observations that proaerolysin can be converted into aerolysin by proteases provided by the host cell (14).[2]

These observations show that proaerolysin and aerolysin are able to bind to HL-60 cells and that the cells express proteases that can process the protoxin to its mature form. This allows heptamerization of the toxin and channel formation thereby leading to efflux of intracellular potassium, presumably to concomitant sodium entry, and membrane depolarization.

*Aerolysin Induces $[Ca^{2+}]_c$ Elevations Which Display Complex Kinetics*—To investigate whether the interaction of aerolysin with myeloid cells led to changes in cytosolic free $Ca^{2+}$ concentration ($[Ca^{2+}]_c$), we exposed fura-2 loaded HL-60 promyelocytes and HL-60 granulocytes to either proaerolysin or trypsin-activated aerolysin (Fig. 3). Both, the protoxin and the mature toxin induced elevation of $[Ca^{2+}]_c$ in a dose-dependent manner and this in both cell types. The kinetics of the $[Ca^{2+}]_c$ increase were, however, markedly faster when the mature toxin was added rather than its precursor as previously observed for membrane depolarization (Fig. 3, *A* and *C versus B* and *D*). Also, the effects of both the pro and the mature toxin were more pronounced on the differentiated granulocytic HL-60 cells then on the immature promyelocytic cells. No changes in $[Ca^{2+}]_c$ could be observed upon addition of the hemolytically inactive G202C/I445C mutant when added either in the pro or the mature form (Fig. 3*D*).

A striking feature of the aerolysin-induced $[Ca^{2+}]_c$ elevations was their complex kinetics. Rather than presenting a monophasic increase, as might be expected for the insertion of a pore into the membrane, the kinetics were multiphasic: an initial,

[2] ■. Abrami, M. Fivaz, and F. G. van der Goot, unpublished data.

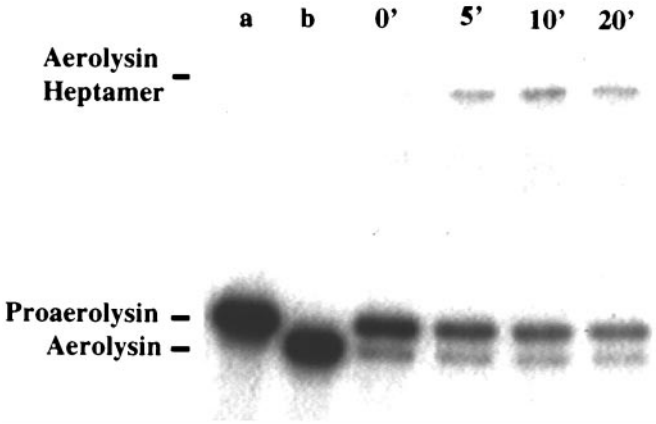


FIG. 2. **HL-60 granulocytes express proteases able to convert proaerolysin to its active form.** HL-60 granulocytes were incubated with 50 ng/ml $^{125}$I-proaerolysin in $Ca^{2+}$ medium for 25 min at 4 °C and washed twice with toxin free $Ca^{2+}$ medium. Cells were then incubated for the indicated times at 37 °C in a toxin-free medium. *a*, proaerolysin marker; *b*, aerolysin marker, other lanes are labeled according to the incubation time at 37 °C. Approximately 300,000 cells were loaded per well. Note that although the complex is not covalent, the aerolysin heptamer is not dissociated by SDS and thus migrates at a high molecular weight.

relatively rapid phase of $[Ca^{2+}]_c$ change was followed by a more sustained phase.

Thus, the toxin-induced $Ca^{2+}$ response in myeloid cells was dose-dependent, accelerated by preactivation of the toxin, and depended on the state of differentiation of the cells. As the responses were most pronounced in HL-60 granulocytes stimulated with the mature toxin, these conditions were used to further analyze the mechanisms underlying the complex $[Ca^{2+}]_c$ response to aerolysin.

*Aerolysin Induces $Ca^{2+}$ Release from Intracellular Stores*—To investigate the source of the aerolysin-induced $[Ca^{2+}]_c$ elevations, we exposed HL-60 granulocytes to aerolysin in a $Ca^{2+}$-free medium. Under these conditions only $Ca^{2+}$ release from intracellular stores can be detected, but not $Ca^{2+}$ influx across the plasma membrane. As shown in Fig. 4*A*, aerolysin (100 ng/ml) was able to induce $[Ca^{2+}]_c$ elevations in a $Ca^{2+}$-free medium, demonstrating that the toxin triggered $Ca^{2+}$ release from intracellular stores. The observed $[Ca^{2+}]_c$ elevations had complex kinetics. An initial phase peaked and decayed after approximately 40–60 s. A prolonged phase which increased toward a plateau could be observed 1–3 min after toxin addition. The binding competent, insertion-incompetent mutant G202C/I445C did not induce $Ca^{2+}$-release (Fig. 4*A*). However, when added in excess, the mutant was able to preclude $Ca^{2+}$ release in response to wild type aerolysin (Fig. 4*B*) confirming that the two variants of the toxin have the same acceptor sites on the cell and that they are limited in number.

Many agonists induce $Ca^{2+}$ release from intracellular stores through phospholipase C (PLC)-mediated Ins(1,4,5)$P_3$ generation and Ins(1,4,5)$P_3$-induced $Ca^{2+}$ release from intracellular stores. To test whether PLC activation is involved in the aerolysin-induced $Ca^{2+}$ release from intracellular stores, we have used the PLC inhibitor U73122. As shown in Fig. 4*C*, this compound inhibited the initial phase of the aerolysin-induced $Ca^{2+}$ release, however, neither the late phase of the $Ca^{2+}$ release, nor the $Ca^{2+}$ influx observed after $Ca^{2+}$ readdition were affected.

*Aerolysin Activates Pertussis Toxin-sensitive G-proteins*—For many granulocyte agonists, $Ca^{2+}$ release from intracellular stores is due to a G-protein-mediated activation of phospholipase C. In contrast to what is observed on many other cellular systems, agonist-PLC coupling in leukocytes is generally mediated by pertussis toxin-sensitive G-proteins (26). We therefore investigated the effect of pertussis toxin pretreatment on aerolysin-induced $Ca^{2+}$ release in the HL-60 granulocytes. As shown in Fig. 5, pertussis toxin pretreatment inhibited the initial, rapid phase of aerolysin-induced $Ca^{2+}$ release (Fig. 5*D*), but not the second, slower, phase (Fig. 5*E*), nor the calcium entry across the plasma membrane. These results demonstrate an activation of pertussis toxin-sensitive G-proteins through aerolysin. The results obtained with pertussis toxin (Fig. 5) and the PLC inhibitor (Fig. 4), however, also demonstrate that there is a second phase of $Ca^{2+}$ release which does not involve the G-protein/PLC/Ins(1,4,5)$P_3$ pathway.

*Aerolysin Released $Ca^{2+}$ from Thapsigargin and Agonist-sensitive $Ca^{2+}$ Stores*—A variety of intracellular organelles are able to serve as intracellular $Ca^{2+}$ stores, the functionally most important of which is thought to be the endoplasmic reticulum (ER). The ER can be subdivided into agonist-sensitive and agonist-insensitive $Ca^{2+}$ stores. The ER $Ca^{2+}$ stores are, in most cases, loaded through $Ca^{2+}$ pumps which belong to the group of the so-called SERCAs (sarcoendoplasmic reticulum $Ca^{2+}$-ATPases). All sarcoendoplasmic reticulum $Ca^{2+}$-ATPases known to date can be inhibited by thapsigargin and are also the only known target of this drug. In addition, this compound efficiently empties ER-type $Ca^{2+}$ stores in many cell types. We therefore investigated the effect of depletion of ER-type $Ca^{2+}$ stores through thapsigargin on the aerolysin-induced $Ca^{2+}$ signal. As shown in Fig. 6*A*, thapsigargin led, as expected, to a transient increase in $[Ca^{2+}]_c$ (Fig. 6*A*, see also Ref. 27). When aerolysin was added to cells after thapsigargin treatment, both phases of the aerolysin-induced $Ca^{2+}$ release were almost completely abolished. Thus, the source of $Ca^{2+}$ released by aerolysin was the endoplasmic reticulum. Thapsigargin did, however, not inhibit channel formation by aerolysin since $Ca^{2+}$ entry and rapid release of intracellular $K^+$ were still observed.

To investigate whether aerolysin induces $Ca^{2+}$ release from agonist-sensitive stores, we stimulated cells with the receptor agonist fMet-Leu-Phe (fMLP) in a $Ca^{2+}$-free medium. Under these conditions, $Ca^{2+}$ is released from agonist-sensitive $Ca^{2+}$ stores and these stores remain depleted (23). The predepletion of agonist-sensitive $Ca^{2+}$ stores by fMLP abolished the initial phase, but not the late phase of aerolysin-induced $Ca^{2+}$ release (Fig. 6, *B* and *C*). Thus, the source of the initial phase of aerolysin-induced $Ca^{2+}$ release were agonist-sensitive $Ca^{2+}$ stores, while the source of the second phase also included agonist-insensitive ER-type $Ca^{2+}$ stores.

*Aerolysin Induced $Ca^{2+}$ Influx*—As already visible from Figs. 3 and 4, the effect of aerolysin on $[Ca^{2+}]_c$ also included a major $Ca^{2+}$ influx component. When $Ca^{2+}$ was added to the cells (in a $Ca^{2+}$-free medium) after different times of incubation with aerolysin, a time-dependent increase in the $Ca^{2+}$ permeability was observed, as witnessed by more rapid increase in fura-2 fluorescence (Fig. 7, *A* and *B*). These observations suggest that as more aerolysin pores were formed, the kinetics of $Ca^{2+}$ entry were faster. We then analyzed the kinetics of entry of $Mn^{2+}$, a $Ca^{2+}$ surrogate commonly used to study $Ca^{2+}$ influx pathways. This divalent cation permeates in small quantities through various $Ca^{2+}$ channels; once inside the cell, $Mn^{2+}$ binds with high affinity (~100-fold higher than $Ca^{2+}$) to fura-2, thereby quenching the fura-2 fluorescence. As shown in Fig. 7*B*, the kinetics of $Mn^{2+}$ and $Ca^{2+}$ influxes were very similar. In order to rule out that the increase in divalent cation influx kinetics were due to massive fura-2 release, we measured the amount of extracellular fura-2 as described under "Experimental Procedures." Less then 20% fura-2 was released into the medium after treatment of HL-60 granulocytes with aerolysin (100 ng/

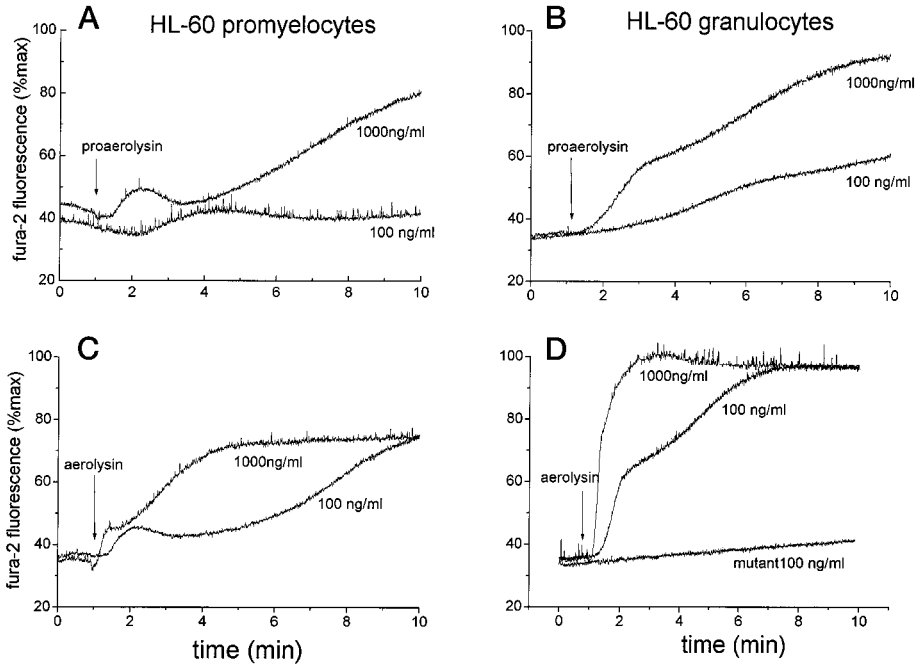


FIG. 3. **$[Ca^{2+}]_c$ elevations in response to proaerolysin and trypsin-activated aerolysin.** $[Ca^{2+}]_c$ was recorded in fura-2-loaded HL-60 promyelocytes (*A* and *C*) and HL-60 granulocytes (*B* and *D*) incubated in $Ca^{2+}$ buffer. At times indicated by an *arrow*, cells were treated with either proaerolysin (*A* and *B*) or trypsin-activated aerolysin (*C* and *D*). All experiments were performed with the wild type toxin, except for the indicated curve in *D*, where the cells were treated with the trypsin-activated G202C/I445C inactive mutant.

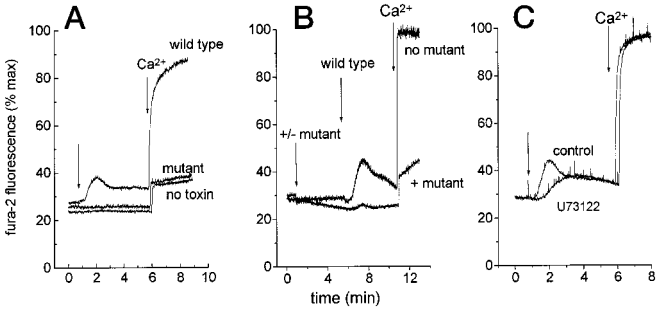


FIG. 4. **Aerolysin-dependent $Ca^{2+}$ release from intracellular stores and $Ca^{2+}$ influx across the plasma membrane.** $[Ca^{2+}]_c$ was recorded in fura-2-loaded HL-60 granulocytes incubated in $Ca^{2+}$-free buffer. However, near the end of each experiment, 1 mM $Ca^{2+}$ was added as indicated. The *unlabeled arrows* indicate the time at which the toxin, mutant or wild type, was added. *A*, addition of wild type aerolysin (100 ng/ml), the inactive mutant G2202C/I445C (100 ng/ml), or buffer (control). *B*, addition of an excess of inactive mutant G2202C/I445C (5 $\mu$g/ml) or buffer (no mutant) was followed by addition of wild type aerolysin (100 ng/ml). *C*, addition of wild type aerolysin (100 ng/ml) to cells that had been preincubated with or without the phospholipase C inhibitor U73122 (2 $\mu$M, 5 min).

ml) during 8 min in agreement with the dye entry kinetics shown in Fig. 1*D*.

Given the fact that aerolysin led to a potassium efflux and plasma membrane depolarization with kinetics similar to the ones observed for divalent cation influx, it is likely that $Ca^{2+}$ enters through the pores formed by the toxin in the plasma membrane. It has indeed been previously suggested that $Ca^{2+}$ is able to diffuse through the aerolysin channel (28). However, given the aerolysin induced $Ca^{2+}$ release from intracellular stores (see above), the toxin could also activate endogenous store-operated $Ca^{2+}$ channels of granulocytes (23). Activation of endogenous channels has been previously suggested for the staphylococcal toxin leukocidin (29). To investigate this possibility, we used the divalent cation $Ni^{2+}$. We have previously shown that this cation blocks store-operated $Ca^{2+}$ influx (27). As shown in Fig. 7*C*, addition of $Ni^{2+}$ to aerolysin-treated cells led to fura-2 quenching indicating that the divalent cation had entered the cells. As a control, Fig. 7*D* shows that $Ni^{2+}$ addition to thapsigargin-treated cells had no effect. Thus, in aerolysin-treated cells, divalent cations can enter the cell through the pores formed by the toxin in the plasma membrane. As suspected, neither the aerolysin-induced $Ni^{2+}$ or $Ca^{2+}$ influx was blocked by pertussis toxin, indicating that channel formation in the plasma membrane is G-protein independent (Fig. 5 and not shown).

*Aerolysin-induced $Ca^{2+}$ Release Occurs After a Lag Time*—Fig. 8 shows, with high resolution, the kinetics of aerolysin-induced $Ca^{2+}$ release. Strikingly, there was a substantial lag time between the addition of aerolysin and the onset of $Ca^{2+}$ release in contrast to what is observed upon stimulation with the receptor agonist fMLP. Moreover, the lag time was concentration dependent (Fig. 8*C*). Thus, the marked lag time observed in response to aerolysin clearly differentiated $Ca^{2+}$ release in response to the toxin from $Ca^{2+}$ release in response to typical receptor agonists.

*Effect of Digitonin, Staphylococcal α-Toxin, and Streptolysin O on Intracellular $Ca^{2+}$*—To further understand the mechanism of G-protein activation by aerolysin, we studied $Ca^{2+}$ signaling by other widely used cell permeabilizing agents such as digitonin, staphylococcal α-toxin, and streptolysin O. Digitonin is a plant lipid which, at low concentrations preferentially binds to cholesterol and thereby leads to plasma membrane permeabilization. As shown in Fig. 9*A*, addition of digitonin to fura-2-loaded cells suspended in a $Ca^{2+}$-free medium led to a drop in fluorescence intensity. Upon subsequent addition of $Ca^{2+}$ to the extracellular medium, a rapid and large increase in fluorescence was observed. These results indicate that permeabilization was efficient but also that digitonin does not trigger release of $Ca^{2+}$ from intracellular stores. This observation is not so surprising since digitonin has been widely used as a permeabilizing agent in studies on the function of intracellular $Ca^{2+}$ stores in large variety of cell types, including granulocytes (30). Thus, G-protein activation and $Ca^{2+}$ release from intracellular stores are not simply due to cell permeabilization.

Interestingly, however, we found that the two other pore-forming bacterial toxins we have studied, staphylococcal α-toxin and streptolysin O, both induced $Ca^{2+}$ release from intracellular stores (Fig. 9*B*). Moreover, the $Ca^{2+}$ release triggered by both toxins was partly blocked by pertussis toxin (Fig.

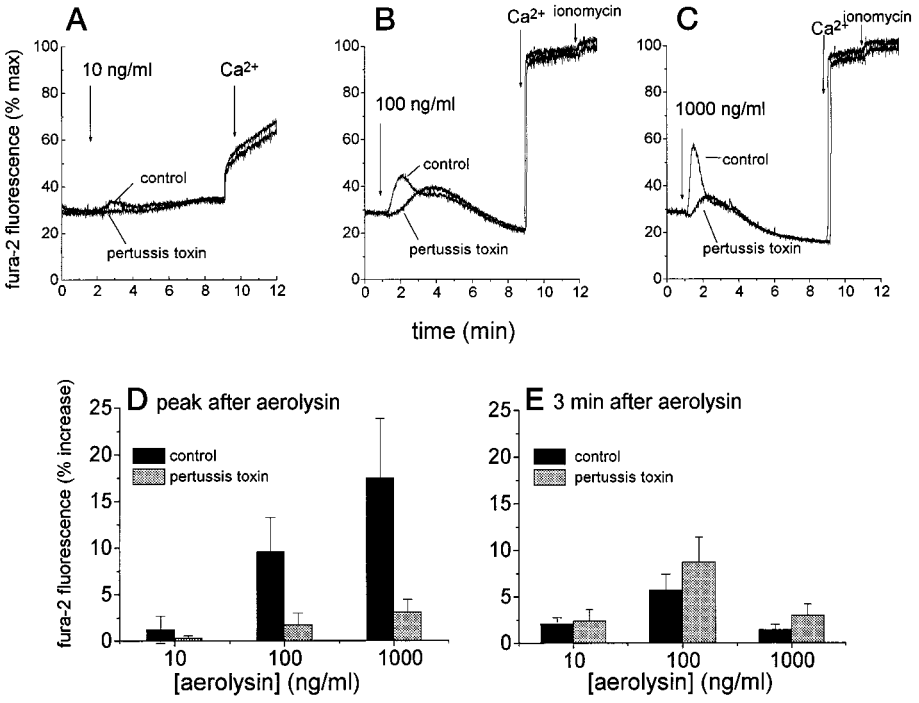


FIG. 5. **Aerolysin-induced $Ca^{2+}$ release from intracellular stores involves pertussis toxin-sensitive G-proteins.** HL-60 granulocytes were pretreated or not with pertussis toxin (500 ng/ml) for 1 h at 37 °C, and subsequently loaded with fura-2 as described under "Experimental Procedures." Cells, suspended in $Ca^{2+}$-free buffer, were then exposed to 10 (*A*), 100 (*B*), or 1000 (*C*) ng/ml of aerolysin at the times indicated by an *arrow*. Near the end of each experiment, $Ca^{2+}$ (1 mM) followed by the calcium ionophore ionomycin (2 $\mu$M) were added as indicated. *D*, percentage of increase in fura-2 fluorescence intensity at the first peak after toxin addition (*i.e.* peak fluorescence minus basal fluorescence) was plotted as function of aerolysin concentration for pertussis toxin treated and control cells. *E*, percentage of increase in fura-2 fluorescence intensity at 3 min after toxin addition (*i.e.* 3-min fluorescence minus basal fluorescence) was plotted as function of aerolysin concentration for pertussis toxin-treated and control cells.

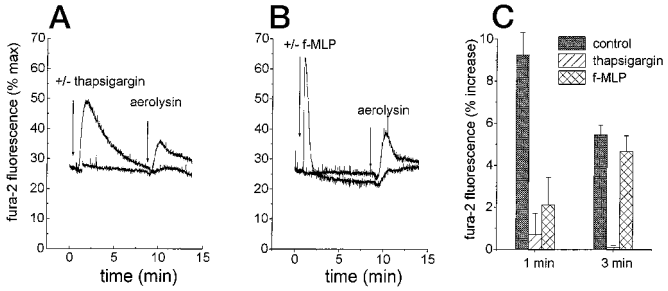


FIG. 6. **Aerolysin leads to the release of $Ca^{2+}$ from thapsigargin and agonist-sensitive stores.** $[Ca^{2+}]_c$ was recorded in fura-2-loaded HL-60 granulocytes incubated in $Ca^{2+}$-free buffer. *A*, addition of the $Ca^{2+}$-ATPase inhibitor thapsigargin (100 nM) or the equivalent volume of $Me_2SO$ (*first arrow*) followed by the addition of aerolysin (100 ng/ml, *second arrow*). *B*, addition of the receptor agonist fMLP (1 $\mu$M) or the equivalent volume of $Me_2SO$ (*first arrow*) followed by the addition of aerolysin (100 ng/ml, *second arrow*). *C*, percentage of increase in fura-2 fluorescence intensity after 1 and 3 min after aerolysin addition in control ($Me_2SO$ treated), thapsigargin, and fMLP-treated cells.

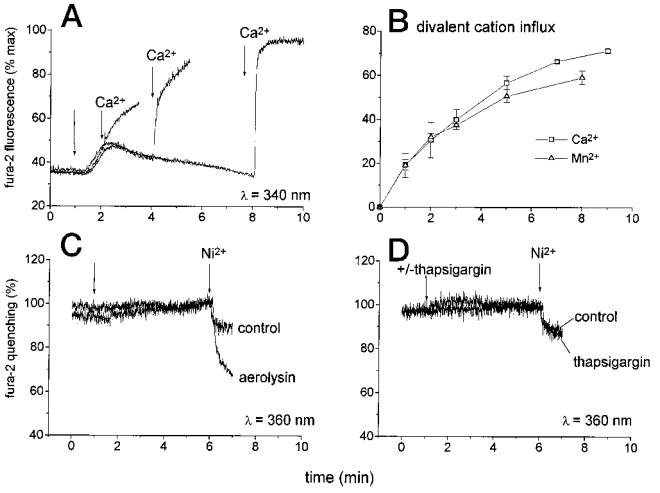


FIG. 7. **Aerolysin-induced influx of divalent cations.** *A*, $[Ca^{2+}]_c$ was recorded in fura-2-loaded HL-60 granulocytes incubated in $Ca^{2+}$-free buffer. The fluorescence was monitored using an excitation wavelength of 340 nm. After different times, $Ca^{2+}$ was added to the extracellular medium (1 mM). *B*, the percentage of fluorescence increase that occurred within 10 s after addition of $Ca^{2+}$ to the extracellular medium was plotted as a function of the time elapse between the addition of aerolysin and the addition of $Ca^{2+}$. Similarly the percentage of fluorescence quenching that occurred within 1 min after addition of $Mn^{2+}$ was plotted as a function of the time elapse between the addition of aerolysin and the addition of $Mn^{2+}$ (25 $\mu$M). *C*, $[Ca^{2+}]_c$ was recorded in fura-2-loaded HL-60 granulocytes incubated in $Ca^{2+}$-free buffer. The fluorescence was monitored using an excitation wavelength $\lambda_{ex}$ of 360 nm, which corresponds to the isosbestic point. The *first arrow* indicates the addition of aerolysin (100 ng/ml) and the second the addition of $Ni^{2+}$ (100 $\mu$M). *D*, $[Ca^{2+}]_c$ was recorded in fura-2-loaded HL-60 granulocytes incubated in $Ca^{2+}$-free buffer ($\lambda_{ex}$ = 360 nm). Thapsigargin (100 nM) was added or not at the *first arrow* and $Ni^{2+}$ (100 $\mu$M) at the *second arrow*.

9*C*) as previously observed for aerolysin. The observation that $\alpha$-toxin triggers $Ca^{2+}$ release is difficult to reconcile with previous reports suggesting that staphylococcal $\alpha$-toxin exclusively triggers $Ca^{2+}$ influx across the plasma membrane (31–33). Note, however, that Suttorp and Habben (31) also did not detect a $[Ca^{2+}]_c$ increase in response to the $Ca^{2+}$ ionophore ionomycin, suggesting that the experimental conditions were not optimized with respect to detection of $Ca^{2+}$ release.

*Pertussis Toxin-sensitive Chemotaxis in Response to Aerolysin, α-Toxin, and Streptolysin O*—To investigate whether toxin-dependent G-protein activation activates cell functions, we investigated the effect of aerolysin, $\alpha$-toxin, and streptolysin O on chemotaxis of freshly prepared human blood granulocytes (Fig. 10). Under control conditions, less then 0.5% of the cells that had been added in the cell reservoir of the chemotaxis chamber were recovered in the target chamber. In contrast, when aerolysin, $\alpha$-toxin, or streptolysin O were added to the target chamber, significant chemotactic activity was observed. The chemotactic activity observed in response to the toxins was of a similar magnitude as observed with classical chemoattractants, such as fMLP or platelet-activating factor (see also legend of Fig. 10). Importantly, chemotaxis in response to the toxins could be completely blocked by preincubation of cells with pertussis toxin, demonstrating that the activation of G-proteins by the toxins was essential for the induction of chemotaxis.

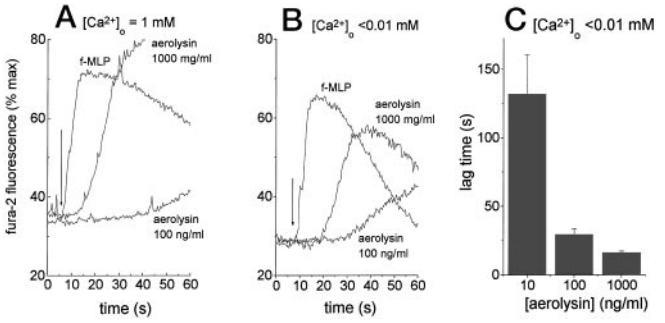


FIG. 8. **Kinetics of early changes in fura-2 fluorescence upon aerolysin or fMLP treatment.** HL-60 granulocytes were incubated in $Ca^{2+}$ (*A*) or $Ca^{2+}$-free (*B*) buffer and the kinetics of increase in fura-2 fluorescence upon addition of aerolysin or fMLP were compared. *C*, the lag time between toxin addition and the onset of the rise in fura-2 fluorescence was measured for various aerolysin concentrations.

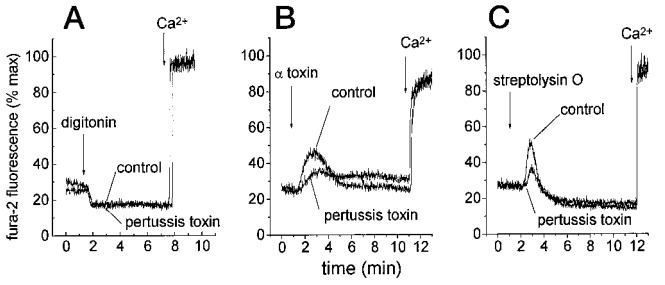


FIG. 9. **Effect of membrane permeabilizing agents on the $[Ca^{2+}]_c$.** HL-60 granulocytes were incubated in $Ca^{2+}$-free buffer. The changes in fura-2 fluorescence were monitored upon addition of digitonin (*A*, 12.5 $\mu$M), staphylococcal $\alpha$-toxin (*B*, 10 $\mu$g/ml), and streptolysin O (*C*, 50 ng/ml). Near the end of each experiment, $Ca^{2+}$ (1 mM) was added as indicated.

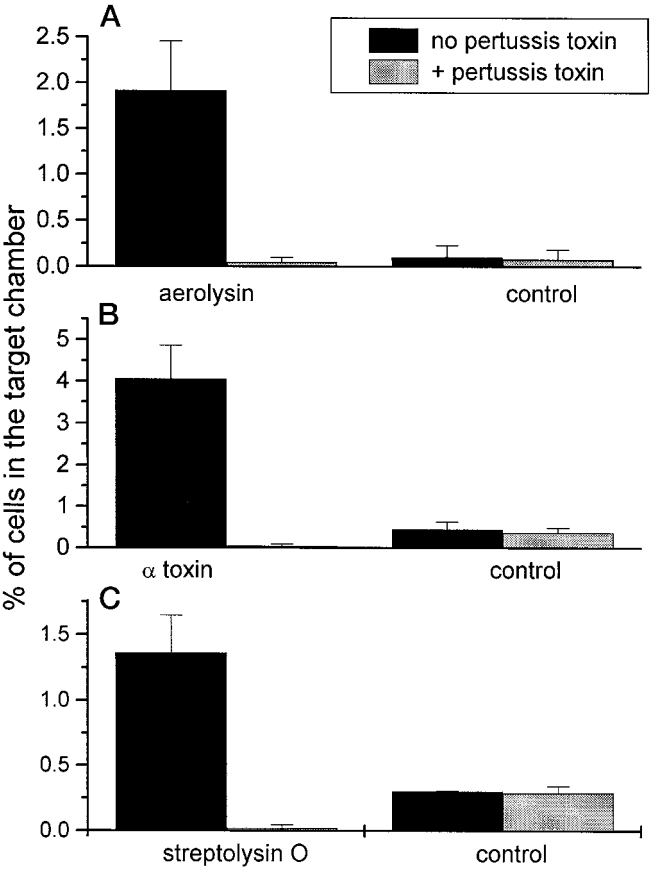


FIG. 10. **Pertussis toxin-sensitive chemotaxis in response to pore-forming toxins.** Chemotaxis of freshly prepared human blood granulocytes in response to aerolysin (*panel A*), staphylococcal $\alpha$-toxin (*panel B*), or streptolysin O (*panel C*) was assessed using a standard chemotaxis assay. Cells were preincubated for 1 h without pertussis toxin (*black bars*) or with pertussis toxin (*gray bars*). For control conditions, toxins were omitted from the target chamber. Data are expressed as % of cells recovered from the target chamber (mean ± S.E.; $n = 3$). Using the same assay system, chemotactic responses to standard chemoattractants were 1.5 ± 1.0% (1 nM fMLP) and 3.2 ± 2.3 (100 ng/ml platelet activating factor).

## DISCUSSION

*A. hydrophila* may cause pyogenic infections, including fecal leukocyte-positive diarrhea and purulent soft tissue infection. An important pathogenicity factor of this bacterium is the pore-forming toxin aerolysin. Thus, the question whether granulocytes are target cells for aerolysin is relevant. In this study, we demonstrate that granulocytes are sensitive to aerolysin. We found that granulocytes are more sensitive than promyelocytes suggesting that an up-regulation of receptors may occur upon differentiation. We also show that granulocytes are able to proteolyticaly activate the protoxin thereby allowing heptamerization of the toxin and channel formation as witnessed by a loss of intracellular $K^+$ and plasma membrane depolarization. Finally we show that aerolysin induces $[Ca^{2+}]_c$ elevations. In agreement with a previous study (34), we also demonstrate that aerolysin is chemotactic for human granulocytes. However, our results not only define an aerolysin target cell of potential pathophysiological importance. They also reveal novel and unexpected aspects of the mechanisms of cell activation by the toxin, namely aerolysin-induced $Ca^{2+}$ release from intracellular stores and aerolysin-induced G-protein activation.

*Aerolysin-induced $Ca^{2+}$ Release from Intracellular Stores*—A pore-forming toxin is expected to allow ion fluxes across the plasma membrane. In accordance with this prediction, our results demonstrate that aerolysin increases the plasma membrane permeability for monovalent and divalent cations in granulocytes. However, aerolysin-induced $[Ca^{2+}]_c$ elevations were more complex than anticipated. Experiments performed in the absence of extracellular $Ca^{2+}$ revealed that an early event triggered by aerolysin was the release of $Ca^{2+}$ from intracellular stores. The $Ca^{2+}$ release occurred in two phases. The first phase of aerolysin-induced $Ca^{2+}$ release was rapid and transient. It could be inhibited by pertussis toxin as well as the phospholipase C inhibitor U73122, indicating that it involves the activation of a G-protein and PLC. This phase was also abolished when agonist-sensitive $Ca^{2+}$ stores were predepleted by exposure of cells to the Ins(1,4,5)$P_3$-generating receptor agonist fMLP. Thus, the source of the early phase of aerolysin-induced $Ca^{2+}$ release were most likely Ins(1,4,5)$P_3$-sensitive endoplasmic reticulum $Ca^{2+}$ stores. The second phase of aerolysin-induced $Ca^{2+}$ release was more sustained, but of a relatively low amplitude. It did not occur through a G-protein phospholipase C pathway. This phase was completely abolished by pretreatment of cells with thapsigargin, but only partially by pretreatment with fMLP. Thus, the source of the second phase of $Ca^{2+}$ release most likely comprised not only Ins(1,4,5)$P_3$-sensitive, but also Ins(1,4,5)$P_3$-insensitive endoplasmic reticulum $Ca^{2+}$ stores. The mechanisms underlying the second release phase have as yet to be determined. Generation of a yet unknown signal at the plasma membrane might occur. Alternatively, a direct action of aerolysin on the endoplasmic reticulum might be considered.

*Aerolysin-induced G-protein Activation*—Our results clearly suggest that aerolysin activates pertussis toxin-sensitive G-proteins in granulocytes. This possibility has also been suggested by previous reports on the block of aerolysin-induced granulocyte chemotaxis by pertussis toxin (34). A most

straightforward explanation for the activation of G-proteins by aerolysin would be the following: the aerolysin receptor on granulocytes is a G-protein-coupled receptor and binding of aerolysin to this protein therefore induces G-protein activation. However, for several reasons, we think that this explanation is unlikely. First, the insertion-incompetent G202C/I445C aerolysin mutant efficiently binds to the same cell surface receptors as the wild type toxin, as evidenced by the almost complete block of aerolysin-induced $Ca^{2+}$ release by the preincubation with the mutant. However, the mutant did not induce $Ca^{2+}$ release. Second, the kinetics of increase in $[Ca^{2+}]_c$ were slower than those triggered by the active form of the toxin, suggesting again that pore formation and not binding is crucial for G-protein activation. Third, all proaerolysin receptors identified so far are GPI-anchored proteins and not transmembrane proteins. Finally, the existence of a lag time between the addition of the toxin and the onset of $Ca^{2+}$ release argues against a direct binding to a G-coupled receptor. Indeed no lag is observed upon addition of receptor agonists such as fMLP. Additional evidence that aerolysin-induced G-protein activation is a consequence of pore formation, rather than of receptor binding comes from the observation that G-protein activation is a common theme observed in response to pore formation by a variety of proteins and peptides.

*Is G-protein Activation Commonly Associated with Pore Formation?*—The ability of activating the Ins(1,4,5)$P_3$ pathway is not unique to aerolysin, since both staphylococcal $\alpha$-toxin and streptolysin O were found to trigger $Ca^{2+}$ release (Fig. 9), and to induce chemotaxis (Fig. 10) in a G-protein-dependent manner. Production of Ins(1,4,5)$P_3$ has also been shown to be triggered by two other pore-forming proteins. Grimminger *et al.* (33, 35) have shown that *Escherichia coli* hemolysin (HlyA) leads to phosphoinositide hydrolysis and production of diacylglycerol but the mechanism by which HlyA triggered a G-protein-dependent pathway was not further analyzed (33, 35). The C5b-9 membrane attack complex was also shown to trigger mobilization of calcium from intracellular stores secondary to activation of phospholipase C and production of Ins(1,4,5)$P_3$ (36, 37). Therefore a number of pore-forming proteins seem to be able to induce G-protein activation. However, membrane permeabilization *per se* does not appear to be sufficient since digitonin was unable to trigger $Ca^{2+}$ release. The observation that a variety of pore-forming proteins lead to G-protein activation also argues against the possibility that the common mechanism resides at the receptor binding level. Indeed although the receptors have not been identified for all these toxins, it is clear that they do not share the same acceptor sites on cells. Aerolysin has been shown to bind to GPI-anchored proteins cells (11–14), and streptolysin O to cholesterol (for review, see Ref. 38). Thus, rather than being on the level of toxin-receptor interaction, the G-protein activation through bacterial toxins might be in relationship to their insertion into the plasma membrane. Receptor-independent G-protein activation through plasma membrane insertion of exogenously added cationic amphiphilic neuropeptides and venom peptides has indeed been described previously (39). Our observation that the onset of $Ca^{2+}$ release in response to the toxin was delayed with respect to the onset of $Ca^{2+}$ release in response to a receptor agonist would be compatible with the present hypothesis.

*Acknowledgments*—We are thankful to J. T. Buckley for providing us with the proaerolysin producing strain and the purified proaerolysin mutant G202C/I445C, Beatrix Vecsey-Semjen for giving us $\alpha$-toxin, and M. Kehoe for giving us purified streptolysin O. We are very grateful to Nathalie Madore for going through all the trouble of providing us with an anti-Thy-1 antibody and are thankful to Roger Morris for giving us the antibody. We thank Eduardo Martinez for human T lymphocytes and Hai-Tao He for mouse T lymphocytes.

REFERENCES

1. Donta, S. T., and Haddow, A. P. (1978) *Infect. Immun.* **21,** 989–993
2. Daily, O. P., Joseph, S. W., Coolbaugh, J. C., Walker, R. I., Merrell, B. R., Rollins, D. M., Seidler, R. J., Colwell, R. R., and Lissner, C. R. (1981) *J. Clin. Microbiol.* **13,** 769–777
3. Kaper, J. B., Lockman, H., and Colwell, R. R. (1981) *J. Appl. Bacteriol.* **50,** 359–377
4. Janda, J. M., Bottone, D. J., Sinner, C. V., and Calcaterra, D. (1984) *J. Clin. Microbiol.* **17,** 588–591
5. Chakraborty, T., Hihle, B., Berghauer, H., and Goebel, W. (1987) *Infect. Immun.* **55,** 2274–2280
6. Howard, S. P., and Buckley, J. T. (1982) *Biochemistry* **21,** 1662–1667
7. van der Goot, F., Ausio, J., Wong, K., Pattus, F., and Buckley, J. (1993) *J. Biol. Chem.* **268,** 18272–18279
8. Howard, S. P., and Buckley, J. T. (1985) *J. Bacteriol.* **163,** 336–340
9. van der Goot, F. G., Lakey, J. H., Pattus, F., Kay, C. M., Sorokine, O., Van Dorsselaer, A., and Buckley, T. (1992) *Biochemistry* **31,** 8566–8570
10. Gruber, H. J., Wilmsen, H. U., Cowell, S., Schindler, H., and Buckley, J. T. (1994) *Mol. Microbiol.* **14,** 1093–1101
11. Nelson, K. L., Raja, S. M., and Buckley, J. T. (1997) *J. Biol. Chem.* **272,** 12170–12174
12. Cowell, S., Aschauer, W., Gruber, H. J., Nelson, K. L., and Buckley, J. T. (1997) *Mol. Microbiol.* **25,** 343–350
13. Diep, D. B., Nelson, K. L., Raja, S. M., Pleshak, E. N., and Buckley, J. T. (1998) *J. Biol. Chem.* **273,** 2355–2360
14. Abrami, L., Fivaz, M., Buckley, J. T., Parton, R. G., and van der Goot, F. G. (1998) *J. Cell. Biol.* **140,** 525–540
15. Garland, W. J., and Buckley, J. T. (1988) *Infect. Immun.* **56,** 1249–1253
16. Wilmsen, H. U., Pattus, F., and Buckley, J. T. (1990) *J. Membr. Biol.* **115,** 71–81
17. Wilmsen, H. U., Leonard, K. R., Tichelaar, W., Buckley, J. T., and Pattus, F. (1992) *EMBO J.* **11,** 2457–2463
18. Moniatte, M., van der Goot, F. G., Buckley, J. T., Pattus, F., and Van Dorsselaer, A. (1996) *FEBS Lett.* **384,** 269–272
19. Buckley, J. T. (1990) *Biochem. Cell Biol.* **68,** 221–224
20. van der Goot, F. G., Hardie, K. R., Parker, M. W., and Buckley, J. T. (1994) *J. Biol. Chem.* **269,** 30496–30501
21. Laemmli, U. K. (1970) *Nature* **227,** 680–685
22. Kasner, S. E., and Ganz, M. B. (1992) *Am. J. Physiol.* **262,** F462–F467
23. Demaurex, N., Monod, A., Lew, D., and Krause, K.-H. (1994) *Biochem. J.* **297,** 595–601
24. Schlossman, S. F., Boumsel, L., Gilks, W., Harlan, J. M., Kishimoto, T., Morimoto, C., Ritz, J., Shaw, S., Silverstein, R., Springer, T., Tedder, T. F., and Todd, R. F. (1995) *Leukcocyte Typing V. White Cell Differentiation Antigens*, p. 154, Oxford University Press, Oxford
25. Papini, E., Sandona, D., Rappuoli, R., and Montecucco, C. (1988) *EMBO J.* **7,** 3353–3359
26. Krause, K. H., Schlegel, W., Wollheim, C. B., Andersson, T., Waldvogel, F. A., and Lew, P. D. (1985) *J. Clin. Invest.* **76,** 1348–1354
27. Demaurex, N., Lew, D. P., and Krause, K. H. (1992) *J. Biol. Chem.* **267,** 2318–2324
28. Tschödrich-Rotter, M., Kubitscheck, U., Ugochukwu, G., Buckley, J., and Peters, R. (1996) *Biophys. J.* **70,** 723–732
29. Staali, L., Monteil, H., and Colin, D. A. (1998) in *Bacterial Protein Toxins* (Fehrenbach, F. J., ed) Vol., Gustave Fisher Verlag, in press
30. Prentki, M., Wollheim, C. B., and Lew, P. D. (1984) *J. Biol. Chem.* **259,** 13777–13782
31. Suttorp, N., and Habben, E. (1988) *Infect. Immun.* **56,** 2228–2234
32. Fink, D., Contreras, M. L., Lelkes, P. I., and Lazarovici, P. (1989) *Cell. Signalling* **1,** 387–393
33. Grimminger, F., Rose, F., Sibelius, U., Meinhardt, M., Potzsch, B., Spriestersbach, R., Bhakdi, S., Suttorp, N., and Seeger, W. (1997) *J. Immunol.* **159,** 1909–1916
34. Jin, G.-F., Chopra, A. K., and Houston, C. W. (1992) *FEMS Microbiol. Lett.* **98,** 285–290
35. Grimminger, F., Sibelius, U., Bhakdi, S., Suttorp, N., and Seeger, W. (1991) *J. Clin. Invest.* **88,** 1531–1539
36. Morgan, B. P., and Campbell, A. K. (1985) *Biochem. J.* **231,** 205–208
37. Cybulsky, A. V., Salant, D. J., Quigg, R. J., Badalamenti, J., and Bonventre, J. V. (1989) *Am. J. Physiol.* **257,** F826–F836
38. Bhakdi, S., Bayley, H., Valeva, A., Walev, I., Walker, B., Kehoe, M., and Palmer, M. (1996) *Arch. Microbiol.* **165,** 73–79
39. Mousli, M., Bueb, J. L., Bronner, C., Rouot, B., and Landry, Y. (1990) *Trends Pharmacol. Sci.* **11,** 358–362